Environmental Science and Pollution Research (2022) 29:29510–29523
https://doi.org/10.1007/s11356-021-17211-0

THE INTERACTION BETWEEN ENVIRONMENTAL POLLUTION AND CULTURAL HERITAGE: FROM OUTDOOR TO INDOOR

Conservation state of two paintings in the Santa Margherita cliff cave: role of the environment and of the microbial community

Francesco Armetta[1] · Josue Cardenas[1] · Eugenio Caponetti[1,2] · Rosa Alduina[1] · Alessandro Presentato[1] · Luca Vecchioni[3] · Pietro di Stefano[4] · Alberto Spinella[5] · Maria Luisa Saladino[1]

Received: 15 February 2021 / Accepted: 21 October 2021 / Published online: 9 November 2021

Abstract

The conservation of ancient paintings sited in humid environments is an actual challenge for restorers, because it needs the knowledge of the materials the paintings are made up and of their interaction with a peculiar surrounding environment; thus, tailored procedures and strategies aimed at restoring and preserving paintings are necessary. Santa Margherita's cave in Castellammare del Golfo (Trapani, Italy) is a natural cave, containing the remains of paintings, in a poor state of conservation, belonging to an ancient church dated back to the Middle Age. The present manuscript reports the monitoring of environmental conditions (i.e., temperature and humidity) in a full year, as well as a study on the materials constituting the stone support and the paintings together with a survey of the microbial community. The findings allow us to define the causes that mainly involve the degradation of the paintings. In detail, the degradation of the east and the west walls occurred differently because of the exposure to the sea aerosol, which influenced the salt composition, also contributing to diversifying the bacterial community. Some specific actions to plan the conservation and restoration of paintings and to preserve the site are suggested.

Keywords Cave painting · Sulfates and chlorides · Bacterial community · Environmental monitoring · Conservation plan

Introduction

Since prehistory, caves have represented natural shelters for both animals and human beings, featuring traces of their activities that need to be preserved as a potential source of information inherited by modern society. Occasionally, caves could be artificially modified by either building defense walls or decorating them with paintings, depending on the cave's use (Aubert et al. 2018). In the case of shrines or churches, there are plenty of sites that contain paintings of high artistic relevance (Metin and Soslu 2018; Tascon et al. 2017). From a geological perspective, sicilian territory is characterized by karst landforms (typically featuring underground quarries), therefore composed of sedimentary layers (i.e., cutters, sinks, and caves), resulting from geomorphic processes due to the chemical solubility of rocks in both ground and surface water. Due to high religious influences during the Medieval Age, several sicilian caves have been used as churches such as Grotta di Santa Margherita, Parpadura Sanctuary, Grotta dei Santi, Grotta del Crocifisso, Grotta di Santa Rosalia, and Grotta di San Mauro to name a few. In many cases, these environmental settings feature

Responsible Editor: Michel Sablier.

✉ Francesco Armetta
francesco.armetta01@unipa.it

✉ Alessandro Presentato
alessandro.presentato@unipa.it

[1] Dipartimento Scienze E Tecnologie Biologiche, Chimiche E Farmaceutiche - STEBICEF, Università Di Palermo, Viale delle Scienze Ed.16 and 17, 90128 Palermo, Italy

[2] Labor Artis C.R. Diagnostica S.R.L, Via Celona, Palermo, Italy

[3] Dipartimento Scienze E Tecnologie Biologiche, Chimiche E Farmaceutiche - STEBICEF, Università Di Palermo, Via Archirafi, 18, 90123 Palermo, Italy

[4] Dipartimento Scienze Della Terra E del Mare, Università Di Palermo, Via Archirafi, 22, I-90123 Palermo, Italy

[5] ATeN Center, University of Palermo, Viale delle Scienze Ed.18, 90128 Palermo, Italy

the presence of precious paintings, as evidence of the piety and arts in the territory, and especially for small regions, these works of art represent a great economical source and cultural identification. The conservation of ancient paintings sited in humid environments is a continuous challenge because of the different nature and heterogeneity of materials to be preserved. Therefore, it is crucial to deepen the knowledge about the processes involving deterioration and surface modification of such materials. Several studies reported on analyses of paintings to get information about their production and conservation state (Russ et al. 2017; Creer and Kopper 1974; La Russa et al. 2016; Vettori et al. 2016), as well as biological aspects responsible for biodeterioration phenomena (Caneva et al. 2019; Zhang et al. 2019; Piacenza et al. 2020); others demonstrated the importance of the environmental monitoring and the study of processes involved during the decay of different kind of materials (Lee et al. 2019; Nason and Lithgow 1999; Scatigno et al. 2016; Belfiore et al. 2013). Particularly, biodeterioration phenomena have a great impact on rock settlements due to favorable environmental conditions such as condensation phenomena and enrichment of salts and organic materials, which can favor the growth of organisms. This aspect frequently leads to the thriving of autochthonous microorganisms as biofilms that can affect, from an aesthetic and structural perspective, the "integrity" of mural paintings (Nugari et al. 2009). In this regard, it is also worth noting that biological activities are responsible for the production, under certain environmental conditions, of bioactive compounds, whose action, in determining physical–chemical damages of rock materials, cannot be neglected. Moreover, considering the importance of the microflora-to-environment occurring relationship, it is advisable to consider ecological approaches when it comes to the diagnostic of the conservation state of a given site, therefore allowing to wisely plan a preventive conservation design (Caneva et al. 2017). In this study, both physical–chemical and biological approaches have been applied to gain valuable information about materials constituting the stone support and paintings of the Santa Margherita's cave in Castellammare del Golfo (Trapani, Italy), as well as to survey for the bacterial community present on the east and west walls of this natural environment. Besides, a full-year monitoring of the environmental conditions (i.e., temperature and humidity) of the cave contributed to unveil processes involving degradation phenomena. Thus, based on the information gathered at the multidisciplinary level, the goal of the investigation is to define the conservation state of the paintings and to plan restoration actions aimed to preserve both wall paintings and the site.

The site

The Santa Margherita's cave is a karstic cave probably overprinted by marine erosion during Pleistocene times, being located on a coastal cliff in front of the sea (coordinates, Latitude: 38.036601 and Longitude: 12.871712) at an altitude of 10 m above the sea level. This cave represents an ideal case study evaluating parameters involving degradation processes of the wall painting, as the presence of salts is one of the main causes of deterioration of art objects featuring a porous nature, particularly wall paintings and stone statues (Charola 2000).

According to the description of Galante (Galante 2011), the paintings correspond to the Byzantine style from the twelfth Century (Purpura 1999), being located in both east and west walls and featuring a different degree (Fig. 1).

The original east wall painting was ca. 27 m^2 in size, while the remains extend only for 9 m^2 towards the entrance of the cave. Although most of the wall painting is lost, it is clear the representation of Christ's crucifixion on a frame of 0.40 m^2. The elements show the right side of a human body with an arm over a cross and a feminine figure with her hands clasped to the chest. The rest of the materials show lines and traces of pigments in different colors. The original painting of west wall covered a total dimension up to 36 m^2, yet the remains have been reduced to an area of 22 m^2 towards the entrance of the cave. On this wall, a new layer of painting overlaps the older one. Details of the two paint layers are reported in Figure S1, while some of the main alterations featuring the site are shown in Fig. 3. These alterations can be ascribed to lichens, plants, and water infiltration, which likely come directly from cracks or ascending for capillarity, therefore determining fissures and looseness of the original mortar. Also, human activities contributed to altering the site, being present diverse graffitis such as those painted with pencils, ink, and chalk, as well as engraved (Fig 2).

Methods

Sampling

The analyses of the wall paintings and, therefore, the sampling of the stone support, mortars, and plasters were performed following the principle of minimal invasiveness. Considering that the area of the original paintings is reduced in the time, the sampling was performed considering the border area or lacks. Specifically, 4 samples of stone supports of few centimeters (two for each wall) and 3 samples of mortars of few millimeters with parts of

Fig. 1 Coastal cliff in which the site is located; the entrance of the cave is indicated by a red circle (**a**); detail of the cavities on the surface eroded at the entrance of the cave (**b**); general view of the interior of the cave (**c**), the eastern wall is to the left side of the picture and the western wall to the right

the pictorial layer were collected by using a scalpel (one sample from the east wall and two sets of mortar samples were collected from the two layers of west wall paintings). The samples are indicated with either E or W referring to the east or west wall, respectively, while the material is identified by the letters S (stone) or M (mortar). Since the west wall features two painting layers, the numbers 1 and 2 correspond to the below and upper layers, respectively. Particularly, the sample WM1 contains the pictorial layer with traces of bright red and yellow; therefore, it was considered appropriate to investigate the binder and pigments before the preparation of the cross-section. Figure S2 reports the sampling points of the walls.

Characterization

The monitoring of humidity and temperature was performed along 1 year by placing the EasyLog EL-USB-2 Lascar electronics data loggers on both east and west walls of the cave.

The stone support and mortars were characterized by optical microscopy and X-ray diffractometry to investigate the mineralogical composition and distribution. Thin sectioned samples have been observed through a LEITZ LABORLUX® 12 POL microscope working in polarized and transmitted incident light, which was equipped with binocular phototubes and an automatic digital camera LEITZ VARIO-ORTHOMAT® featuring a rotating stage. X-ray diffraction (XRD) patterns were acquired through a Philips PW 1050/39 diffractometer in the Bragg–Brentano geometry using Ni-filtered Cu Kα radiation ($\lambda = 1.54056$ Å) in the 2θ range 5–90° with a step of 0.05° and an acquisition time of 5 s per step. The X-ray generator worked at a power of 40 kV and a current of 30 mA, and the resolution of the instrument (divergent and antiscatter slits of 0.5°) was determined using R-SiO_2 and R-Al_2O_3 standards free from the effect of reduced crystallite size and lattice defects. The phase identification was performed by using the X'pert HighScore® Software and compared with spectra from the database of the RRUFFTM Project. MAUD was used for the Rietveld analysis of the patterns.

The constituents of the paintings (pigments, inerts, and bindings) were identified by X-ray fluorescence (XRF), (pigments and inerts) and by IR and NMR spectroscopy (bindings). The XRF measurements were performed in situ by placing a portable spectrometer Tracer III SD Bruker AXS in contact with the selected colored area of the painting. The source was a rhodium target X-ray tube operating at 40 kV and 11 mA and an acquisition time of 30 s. The detector was a 10-mm^2 silicon drift X-Flash with Peltier cooling system and a resolution of 145 eV at 100,000 cps. The S1PXRF® Software manages data acquisition. The spectral assignments of the characteristic peaks of an element were carried out using the database contained in the ARTAX 8 software. In each spectrum, the signals of rhodium (Rh) and argon (Ar) due to the source and the atmosphere, respectively, are present. The net area percentages of the identified elements

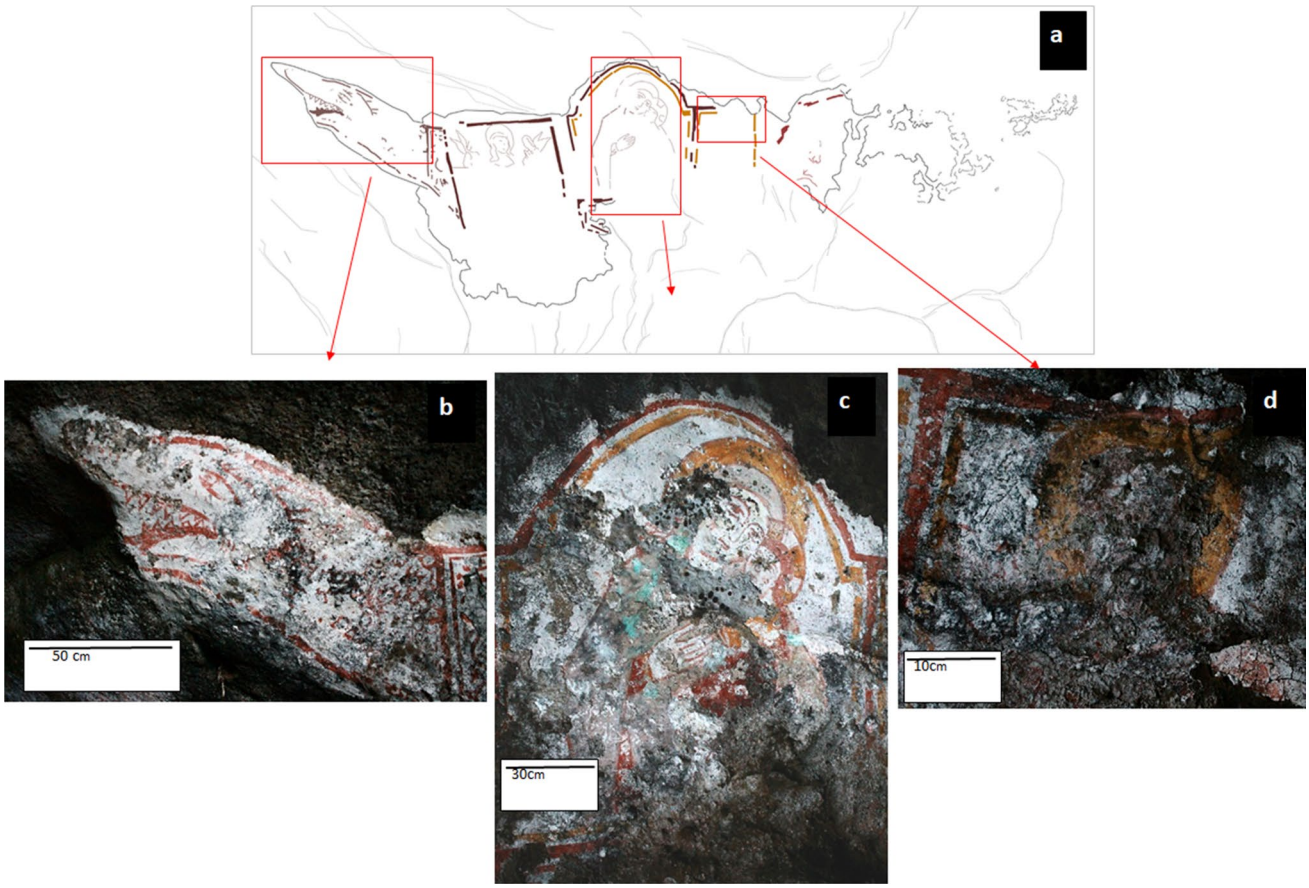

Fig. 2 Map (**a**) and details from the scenes represented on the first layer of painting from the west wall, mostro marino (**b**), Madonna col bambino (**c**), figure not identifiable (**d**)

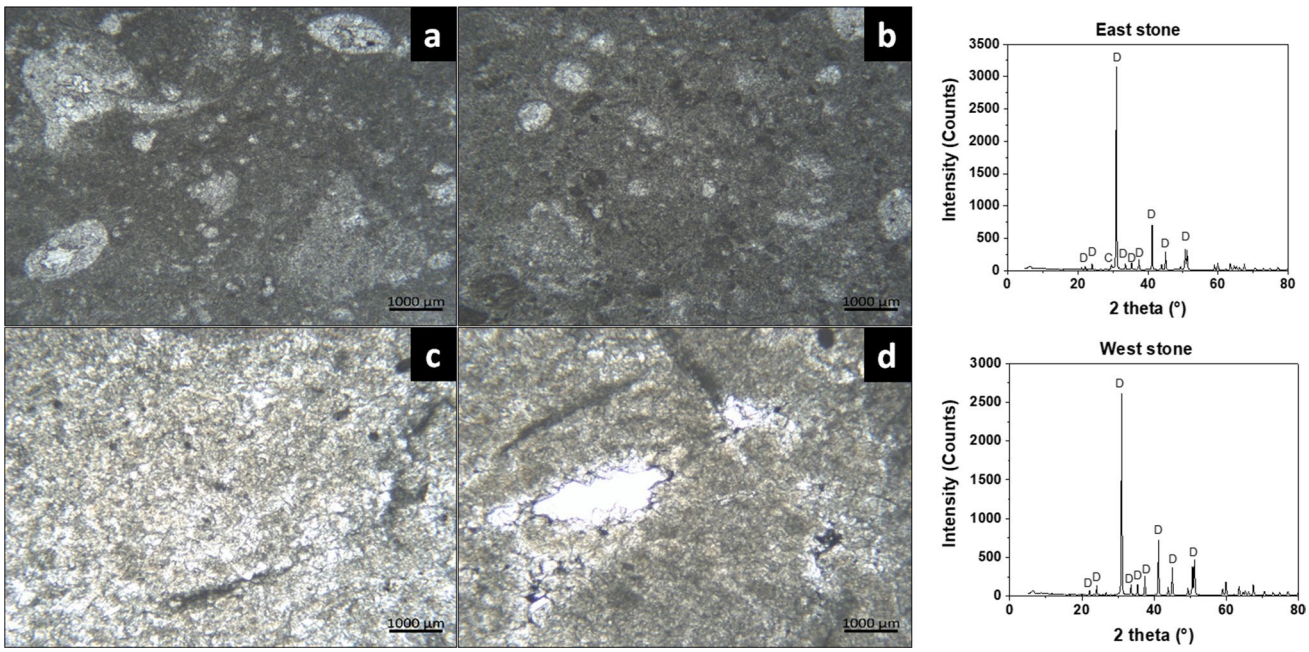

Fig. 3 Microphotographs of the thin sections from east wall (**a**–**b**) and west wall (**c**–**d**). XRD patterns obtained from samples east and west stone (on the right). The crystal phases correspond to dolomite (D) (Ref Code 01–075-1655) and Mg calcite (Ca) (Ref Code 01–086-2335)

were obtained after deconvolution of the peaks, background subtraction, and thus normalized with respect to the total peaks area; results were analyzed through a chemometric approach. For the statistical analysis, the Kα peaks were considered for the elements Si, S, K, Ca, Fe, Cu, As, and Sr. The area percentage was log normalized to equilibrate the contribution of minor and major elements making them comparable. Thus, the principal component analysis (PCA) was applied to all the data (Renda et al. 2019) by using the software Past 4.05 (Hammer et al. 2001). Two different types of equipment for attenuated total reflectance (ATR) were used to perform Fourier-transform infrared spectroscopy (FTIR) measurements. A Bruker Vertex 70 Advanced Research FT-IR Spectrometer equipped with platinum ATR and diamond crystal was used to analyze samples in the 70–4000 cm^{-1} range, with a step of 2 cm^{-1}. The measurements have been performed with 200 scans at 2 hPa on a small amount of powdered sample. A Bruker Micro FT-IR LUMOS spectrophotometer equipped with a germanium crystal was used to analyze samples in the 600–4000 cm^{-1} range, with a step of 2 cm^{-1}. The pigment areas were selected by the microscope magnification, the investigated area corresponding to a few hundreds of microns is due to the crystal tip size. A Bruker VERTEX equipment was used to analyze powders of mortars and μFTIR Bruker LUMOS to analyze pigments. Once the spectra were collected, the analysis of the spectra was done by comparing the results with a database from Vahur et al. (2016) and the investigation of Tortora et al. (2016). ^{1}H NMR spectra and ^{1}H ^{13}C 2D HSQC were obtained at room temperature using a Bruker Avance II 400 (9.4 T) spectrometer operating at 400.15 MHz and 100.62 MHz for the ^{1}H and ^{13}C nuclei, respectively. ^{1}H NMR spectra were performed using a 90° pulse 12.3 us on the proton, a delay time of 5 s, and 128 scans. The ^{1}H ^{13}C 2D HSQC correlation experiments were acquired via double INEPT transfer using Echo/Antiecho – TPPI gradient selection and decoupling during acquisition, 32 scans for 512 experiments.

To recover the organic part of the pigment layer, the sample was subjected to extraction in deuterated acetone by sonication for 45 min. Afterwards, the extract was separated from the insoluble portion by filtration through glass wool and it was placed in a 5-mm NMR tube.

Determination of microbial community

The metagenomic DNA (mDNA) was isolated from stone microsamples of east and west walls, as described elsewhere (Presentato et al. 2020a, 2020b), with some modifications. Briefly, stone materials were soaked in 3 mL of sterile saline solution (NaCl 0.9% w/v) and vigorously shaken (600 rpm) at 30 °C for 2 h. Afterwards, stone materials were carefully removed and NaCl solutions centrifuged (15,000 g) for 30 min at room temperature, generating a biomass pellet that was processed through the chloroform-phenol method to isolate the mDNA. The quality of the mDNA was evaluated by NanoDropTM 2000 spectrophotometer (Thermo Scientific, Waltham, MA, USA), and its suitability was tested by amplifying the 16S rRNA using the universal primer pair F1 and R12 (Coy et al. 2014) with the OneTaq DNA polymerase (NEB) under the following thermal conditions: (i) initial denaturation temperature of 95 °C for 5 min; (ii) run of 30 cycles with each cycle consisting of 30 s at 95 °C (denaturation), 30 s at 50 °C (annealing), and 1 min at 72 °C (extension); and (iii) final extension step at 72 °C for 10 min. The amplification product was visualized by agarose (1% w/v) gel electrophoresis, which showed bands of the expected size (ca. 1500 base pair (bp); data not shown), therefore highlighting the suitability of the as-extracted mDNA for further analyses. The microbiome sequencing was carried out on the internal fragment (ca. 464 bp and corresponding to V3-V4 regions) of the 16S rRNA, which was amplified by using the primer pairs reported elsewhere (Takahashi et al. 2014) and mDNA as a template. The purified polymerase chain reaction products were sequenced by BMR Genomics Srl (Padova, Italy) in one 300 bp paired-end run on an Illumina MiSeq platform. Raw sequences were inferred using DADA2 v.1.8 (Callahan et al. 2016) in order to trim, filter, and remove chimeras and to denoise all sequences, obtaining amplicon sequence variants (ASV). Taxonomical assignment was performed using the SINA classifier on the latest SILVA dataset available (Pruesse et al. 2012) (https://www.arb-111 silva.de/ngs/). Rarefaction analysis was carried out plotting the number of observed ASVs against the total number of filtered reads for each sample.

Results and discussion

Environment monitoring

Humidity and temperature trends registered throughout 1 full year, alongside the corresponding dew point for both walls (Figure S3 of Support Information), indicated how these parameters affected paintings similarly. Specifically, the temperature's trend showed a high variation between September (26 °C) and March (14 °C), while the humidity one featured values ranging from 80 to 50% during summer and wintertime, respectively. The dew point values resulted lower than the registered temperature, indicating the absence of vapor condensation phenomena. Despite the localization in front of the sea, the cave featured a constant environment throughout the year.

Stone support and mortars

East wall microphotographs of stones thin-section from the host rock show the features of dolomitized limestone (Fig. 3a,b). As indicated by the XRD analysis, the sample consists of a small amount of calcite together with dolomite phase (Fig. 3). The Rietveld refinement allows to estimate at about 97% of dolomite and 2.5% of calcite. The carbonate matrix contains fine-grained dolomite crystals and recrystallized bioclasts, probably benthic foraminifer's tests, that appear as small globular grains.

West wall sample (Fig. 3c,d) shows the features of a dolostone. It is composed of a fine to medium crystalline mosaic of dolomite as evidenced by the XRD pattern (Fig. 3e). In this case, the Rietveld refinement confirms that the sample consists of 100% dolomite.

This type of dolomite is formed during diagenetic processes when magnesium-rich groundwaters allow the replacement of calcite ($CaCO_3$) with dolomite crystals $CaMg(CO_3)_2$ (Fairbridge 1957). Both analyzed stone samples corresponded to the same lithological unit and the same diagenetic process. The host rock of the cave belongs to a sedimentary succession of shallow marine carbonates of the Late Triassic age described at the beginning of the past century as "*Dolomia Principale di Castellammare del Golfo.*"

East and west 1 mortars corresponded to a matrix of white color without aggregates distinguishable by the naked eye. The thickness of the layer changes on millimeters according to the surfaces of the wall. West 2 mortar showed a white matrix with different sizes of aggregates not well rounded and featuring diverse color shades (i.e., black, grey, and red). The thickness of the layer ranges from 2 cm to less in different areas of the painting.

The microscopic observation of mortars' cross-sections reveals that east mortar (EM, Fig. 4a) consists of a fine-grained matrix constituted by 90% of binder fraction and 10% of amorphous and well-rounded aggregates with particles size between 5 and 500 µm with colors varying from white to reddish brown. West 1 mortar (W1M, Fig. 4b) similar to east mortar consists of a fine-grained matrix constituted by 85% of binder fraction and 15% of amorphous and rounded aggregates between 5 and 200 µm with colors varying from white to reddish brown. West 2 mortar (W2M, Fig. 4c) consists of a matrix constituted by 60% of binder fraction and 40% of angular and rounded aggregates with particles size between 50 and up to 2 mm. The colors change from white and gray to reddish brown. W2M is thus different from the two others.

To shed more light on differences occurring among mortar samples—potentially ascribed to environmental influences—IR spectroscopy and XRD (Fig. 5) were performed.

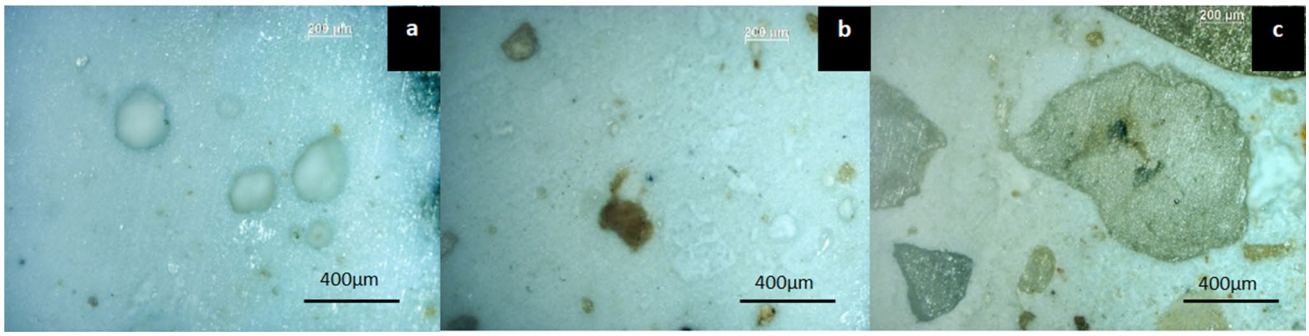

Fig. 4 Photo of samples from east mortar (**a**), west 1 mortar (**b**), and west 2 mortar (**c**) observed under the optical microscope

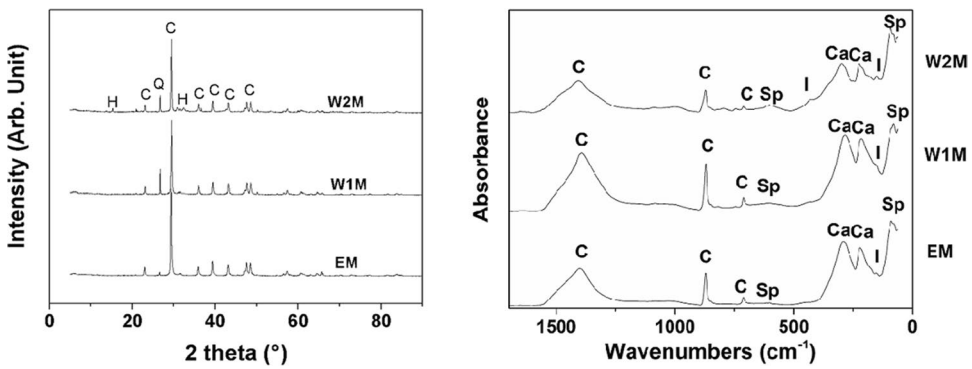

Fig. 5 FTIR spectra of east mortar (EM), west 1 mortar (W1M), and west 2 mortar (W2M) showing the bands associated to calcite (C), other carbonates (Ca), sulfates (Sp), and iron oxides (I). XRD patterns of east mortar (EM), west mortar 1 (WM1), and west mortar 2 (WM2). The crystal phases correspond to calcite (C), hydromagnesite (H), and quartz (Q)

The FTIR spectra of the three samples (Fig. 5a) show the characteristic bands of calcite (713, 874, 1396 cm^{-1}). In addition, the spectra suggest the presence of different compounds based on carbonates (816, 746, 295, 220 cm^{-1}), sulfates (614, 601, 81 cm^{-1}), and iron oxides (432, 150 cm^{-1}). The XRD patterns (Fig. 5b) show that the mineral phases occurring in all the samples correspond to calcite (C), quartz (Q), and hydromagnesite (H). According to the literature, calcite and hydromagnesite are characteristic of the binder fraction, while quartz to the aggregates fraction. Since in coastal regions the atmosphere features particles containing ionic species (mainly chlorides and sulfates) naturally generated due to the action of the wind on the seawater, it is reasonable to suggest that sulfates likely penetrate mortars through ionic diffusion (Salvadori et al. 2003; Rizzo et al. 2008). On the other hand, revealing the presence of gypsum is of utmost importance, as it can influence the mechanical stability of mortars, therefore requiring specific approaches of conservation (Grassi et al. 2007; Carretti et al. 2007; García-Vera et al. 2020; Salvadori et al. 2003).

Pigments and binders

At first glance, pigments featuring east and west 1 paintings were applied through thin layers of brushstrokes, being plane colors and thicker lines characteristic of the utilized style.

In the case of the west 2 painting, the painting style was more developed, as highlighted by the scene representation through veiling and fine lines of pigments, which were inhomogeneously applied on dry plaster, being the thickness of the pigment layer less than 70 µm (Figure S4 of Supporting information).

The investigation of the pigments was performed by the XRF technique, analyzing 45 spots (5 × 5 mm each; Figure S5 of Supporting information). All the spectra presented similar elemental profiles, and, to better highlight the relationship between the elemental composition and the pigment classification, the PCA statistical analysis was carried out on the element area percentages obtained by the profiles deconvolution (Fig. 6).

Red and yellow spots constituted a well-defined group at positive values of PC3. Considering the loadings, it is possible to associate this grouping with the high iron content, likely due to ochres. As for the dark red area, a small group, at the highest PC3 value, in which arsenic contribution is significant (1–2% of net area), could be due to the involvement of realgar or to a different possible preparations of ochres (a detailed analysis of arsenic and iron content for red and yellow pigments is reported in the Supporting information). It is interesting to note the dark red points of the West 2 painting are closer to the yellow points instead of the other dark red, for these points in fact the arsenic peak area is close to zero, highlighting a difference in the pictorial palette of this painting compared to the others. The green spot is out of the 95% ellipse, representing an outlier linked to the high copper content as compared to other spots that did not contain significant signals of this element.

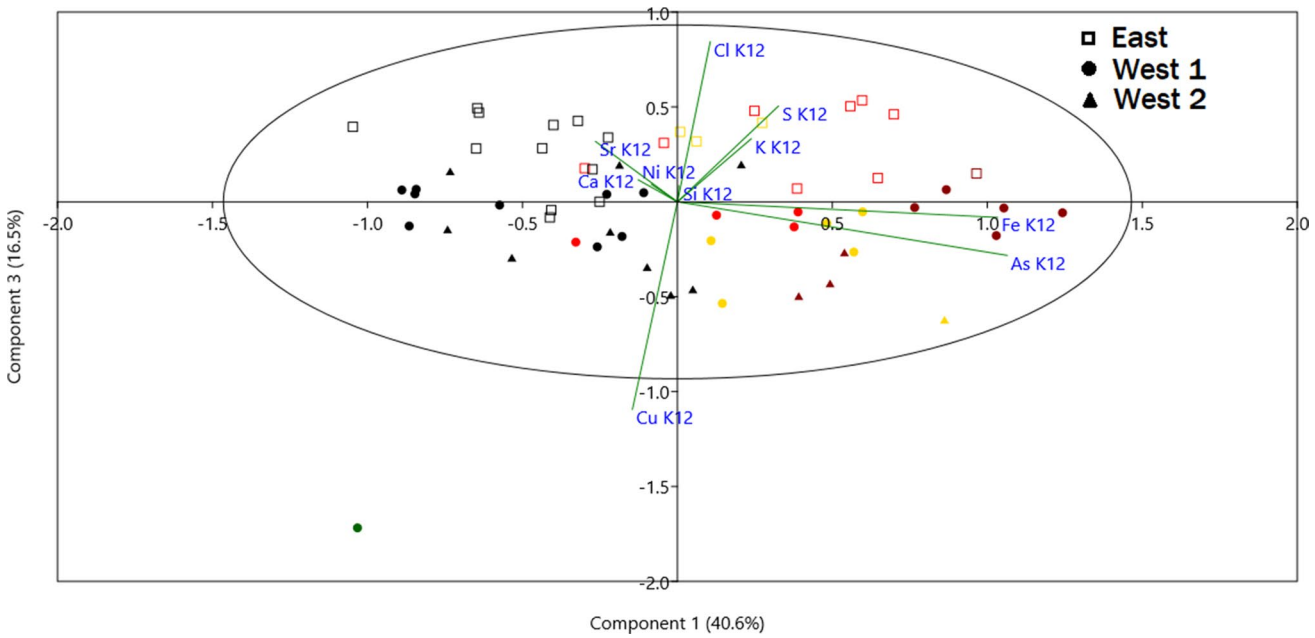

Fig. 6 Projection of principal components (PC1 vs PC3) computed on the log scaled dataset. The score of the analyzed spots red, dark red, yellow, and green were colored in the same way

Table 1 List of colors, chemical elements, and identified pigments

Color	Chemical elements	Pigment
Bright Red	Fe	Red ochre
Dark Red	Fe	Red ochre
Yellow	Fe	Yellow ochre
Pink	Ca, Fe	Mixture of lime white
Grey	Ca, Fe	Mixture of lime white
Green	Cu	Malachite
Black	––	Carbon black

The other colored spots were grouped with the stone and mortar spots at negative PC3 values. In this area of the biplot, the loading contributions came from calcium and strontium elements; thus, for pink and gray colors, the higher peak area of calcium suggested the involvement of either Bianco di San Giovanni or white lime. In the case of the black color, the absence of peculiar XRF signals likely indicates the use of vegetable carbon as a black pigment.

According to these findings, we can hypothesize that the chromatic palette relies on earth pigments also known as ochre or iron oxides (Helen 2003). Since malachite was present in the mantle (usually blue colored) of the Madonna, this pigment could be associated with the conversion of azurite, which generally undergoes degradation because of humidity, as reported by other authors (Saunders and Kirby 2004). For clarity, the color list, chemical elements, and hypothesized pigments are reported in Table 1.

In addition, the XRF investigation highlighted a strong difference in the elements present in the two walls. In detail, the chlorine content and distribution (Figure S7 of the support information) was three times higher (average value 2.6%) in the east wall than the west one (average value 0.8%). This evidence was corroborated by the PCA analysis that grouped all the spots related to the east wall in the positive values of PC1, featuring the loadings of major importance such as chlorine, potassium, and sulfur elements. Since these elements are characteristic of the sea environment, what is reported agrees with the far proximity of the east wall to the marine aerosol exposure, therefore allowing for chlorine salts deposition to occur. Moreover, the interaction of the marine aerosol with building materials enhances their decay processes (Morillas et al. 2020; Comite et al. 2017; Stefanis et al. 2009; Corvo et al. 2010; Costa et al. 2009); thus, it is reasonable to suggest that the marine aerosol is one of the main abiotic causes of deterioration of the east wall painting.

The organic part of the picture layer (binding and varnish) was investigated by IR and NMR spectroscopies. μFTIR spectra (Fig. 7) showed the presence of both inorganic and organic compounds. The bands at 1396, 874, and 713 cm^{-1} were ascribed to the calcite, while the bands at

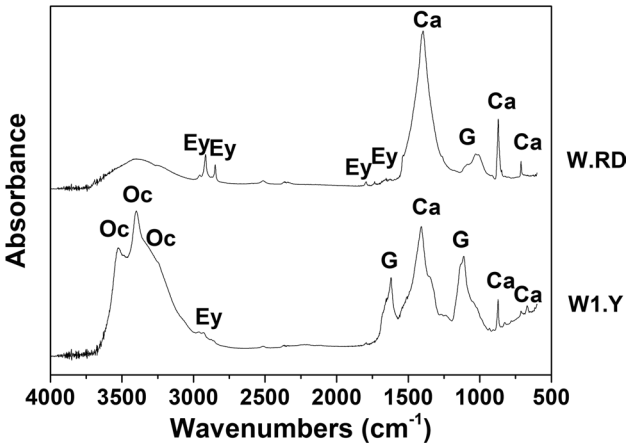

Fig. 7 μFTIR spectra of the yellow pigment (W1.Y) from painting 1 and dark red (W.RD) from the west wall. The bands obtained suggest the presence of calcite (Ca), gypsum (G), Italian gold ochre pigment (Oc), and egg yolk (Ey)

1624, 1105, and 596 cm^{-1} to gypsum, which agrees with the results obtained for the mortars. In addition, the IR spectrum of the yellow color showed the bands at 3524, 3400, and 3240 cm^{-1}, suggesting the presence of the pigment gold ochre (Tortora et al. 2016). The IR spectrum of the dark red color showed bands at 2954, 2918, and 2851 cm^{-1}, which could be due to the presence of egg yolk binder (Tortora et al. 2016; Vahur et al. 2016); the bands at 1792, 1733, and 1716 cm^{-1} could indicate that an oxidation process involving triglycerides of the egg binder took place (Meilunas et al. 1993).

The IR spectra of the yellow samples showed low-intensity bands at the same position previously described.

To confirm the presence of egg yolk used as a binder in the sample collected from the dark red pigment, which had the strongest observable IR bands, ^{1}H NMR analysis was carried out to detect the cholesterol-related signals (Spyros and Anglos 2006; Sofia et al. 2014).

The signals of ^{1}H NMR spectrum (Fig. 8a) at 0.76, 0.87, and 1.01 ppm could be due to the methyl groups of cholesterol. The 2D HSQC experiment results showed that the ^{1}H ^{13}C correlation peaks positions (Fig. 8b), confirming the presence of cholesterol in the analyzed sample. The presence of this molecule, according to Sofia et al. (2014), could be due to the oxidation process involving the fatty acids in the egg binder that, however, does not affect the original carbon skeleton of the cholesterol. Thus, the presence of the cholesterol methyl groups confirmed the use of egg yolk as binding media for paintings.

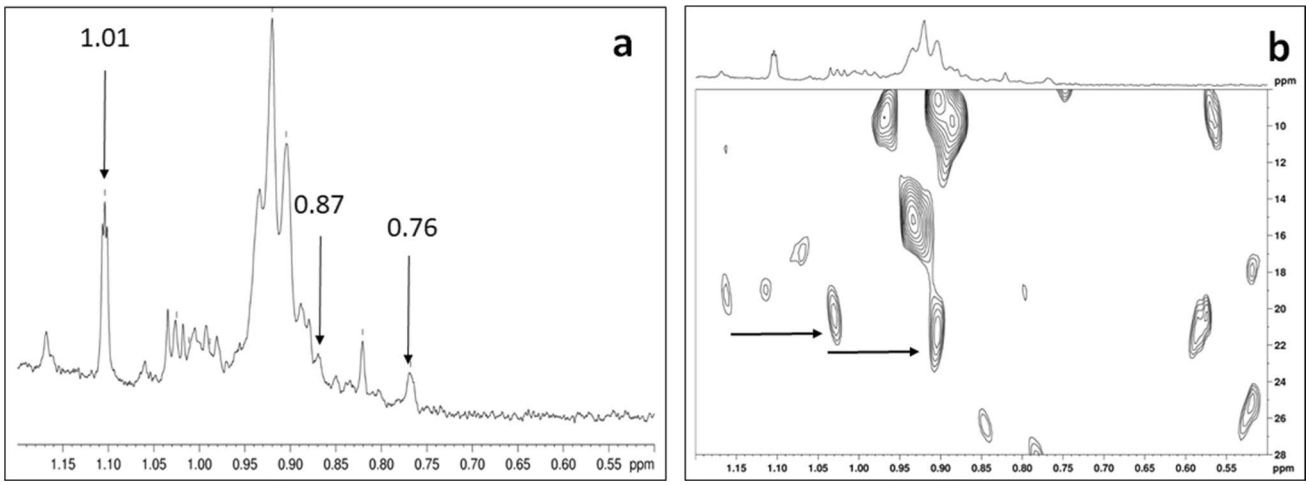

Fig. 8 ^{1}H NMR spectra in acetone-d6 solution of the dark red pigment at magnetic field strength of 400.15 MHz showing peaks of acetone and methyl groups (**a**). Aliphatic methyl region of the 400.15 MHz 1H 2D HSQC NMR spectra of the sample, the arrows indicate the characteristic pattern of the cholesterol methyl groups (**b**)

Microbial characterization

The microbial survey carried out in Santa Margherita's cave was aimed to evaluate the microbial community harbored by this unique environment on one hand and, on the other hand, to give insights about the possible role of microorganisms as a potential risk for paintings conservation. Similarly to what was previously unveiled in related cave environments (Ma et al. 2015; Portillo et al. 2008; Pavlik et al. 2018; Yasir 2018; Alonso et al. 2019), the bacterial community of both east and west walls was represented by Firmicutes, Proteobacteria, Bacteroidetes, Actinobacteria, Cyanobacteria, and Gammatimonodota phyla (Fig. 9a).

Firmicutes, mostly featured by Bacillaceae and Planococcaceae members, was the most represented bacterial phylum

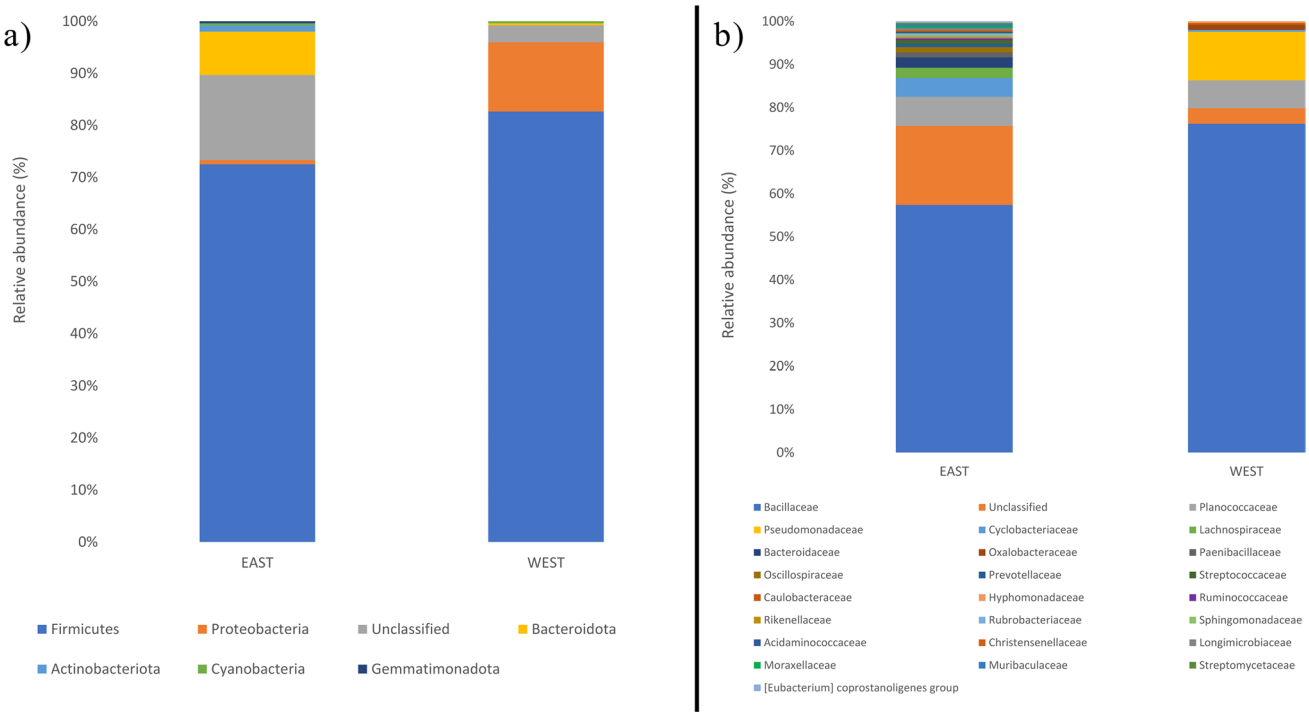

Fig. 9 Relative percentage abundance of bacterial phyla (**a**) and families (**b**) found in the east and west walls of Santa Margherita's cave

found in both walls, accounting for 57% (east) and 76% (west) of the entire microbial community (Fig. 9a), likely due to the capability of these bacterial strains of overcoming the challenge exerted by the abundant minerals such as carbonates ($CaCO_3$) and silicates (SiO_2) (Laiz et al.2000; Randazzo et al. 2015), which were found in Santa Margherita's cave. Indeed, bacilli strains such as *Bacillus pasteurii*, *B. cereus*, and *B. megaterium* (all belonging to the Bacillaceae family), are bacterial members deeply investigated as bioconsolidants of limestone (De Muynck et al. 2013), concrete (Kim et al. 2013; Achal et al. 2011), and plaster (Anne et al. 2010), as result of biotic processes that catalyze the hydrolysis of urea and organic acids (i.e., oxalates and acetates) as carbon and energy sources to support urease activities, which will result in the production of carbonates (Dhami et al. 2014; Dick et al. 2006). Since the bacterial surface is negatively charged, microbial cells can acquire calcium atoms from the surrounding environment, which can precipitate with carbonates forming $CaCO_3$ at the cell surface. Here, the egg yolk used as a binder for the dark red pigment might have represented a source of fatty acids to support bacterial survival in an oligotrophic environment and calcite biomineralization, as reported in the case of *Bacillus subtilis* (Rossi et al. 2006). Moreover, *Bacillus* strains are also able to elicit oxidation reactions (Lu et al. 2010) to deal with the toxicity derived from iron-containing compounds such as iron oxides (Walujkar et al. 2019) and their hydrated forms (Petrushkova and Lyalikova 1986) used as pigments, therefore reinforcing the presence of these bacterial families as a predominant part of the cave's microbial community, as well as a potential risk for conservation of wall paintings.

With a rather low relative percentage abundance (ranging from 1 to 2%), Cyanobacteria phylum was however highlighted in both east and west walls. The growth of these photosynthetic bacteria can be ascribed to the incident natural or artificial light reaching the cave environment, even in the case the amount of incident light is contained over time. Indeed, Cyanobacteria can resist and survive even after a long period of darkness (Albertano 1993; Tomaselli et al. 2000). Specifically, diverse studies demonstrated how environmental parameters (i.e., light and humidity) can determine the growth of photoautotrophic microorganisms on painted surfaces (Pietrini et al. 2008; Roccardi et al. 2008), generating differently colored (e.g., dark green, brilliant green, black, and brown) patinas over wall paintings, as also reported by Nugari and co-workers (2009). Thus, although Cyanobacteria phylum was underrepresented as compared to other bacterial phyla, it cannot be ruled out the biodeteriogenic role played by these bacterial strains, which must be taken into account to better plan actions aimed at preventing colonization events by photosynthetic bacteria.

Despite the higher relative percentage of Firmicutes in the west wall than the east one, the latter displayed a more heterogeneous microbial composition, as were also present—with a relative percentage abundance ranging from 1 to 2% (Fig. 9b)—bacterial members belonging to Lachnospiraceae, Paenibacillaceae, Streptococcaceae, Ruminococcaceae, Oscillospiraceae, Acidaminococcaceae, Christanellaceae, and Eubacteriaceae families, which were not found in the microbial community of the west wall. A similar conclusion can be drawn for Bacteroidota, Actinobacteriota, and Gemmatimonodata phyla (Figs. 8a) that, although a minority, were solely present in the east wall. This aspect, alongside the higher percentage abundance of unclassified bacterial species in the east wall (16%) versus the west one (3%), might be ascribed to the far more proximity of the former to the external cave environment, easily allowing microbial colonization to occur in this area. Another contributing factor could derive from the high chlorine extent found in the east area of the cave, explaining its high microbial heterogeneity in terms of bacterial families such as Paenibacillaceae, Streptococcaceae, Ruminococcaceae, Cyclobacteriaceae, Rubrobacteriaceae, Streptomycetaceae, and Sphingomonadaceae in which are included bacterial strains that can moderately tolerate or even thrive under halophilic conditions (Schabereiter-Gurtner et al. 2001; Remmas et al. 2017; Corral et al. 2020; Chen et al. 2010).

It is also worth noting that some of these bacterial families (i.e., Streptococcaceae, Ruminococcaceae, Moraxellaceae, Streptococcaceae, Oxalobacteraceae, Eubacteriaceae, Sphingomonadaceae, to name a few) are ascribed to the gut microbiota of wildlife (e.g., bat) (Sun et al. 2020; Gaona et al. 2019) that could occasionally use the cave as a shelter, considering that the site entrance is not protected, thus contributing to the microbiota heterogeneity, as well as constituting a potential risk of cave damaging. Thus, microorganisms that can colonize such an environment are likely to be considered as both indigenous and foreign species, which however possess a versatile metabolism, allowing them to thrive under the most disparate nutritional conditions. In this regard, the Proteobacteria phylum mainly inhabited the west area of the cave, reaching a relative abundance of 13% (Fig. 8a). The Gammaproteobacteria family of Pseudomonadaceae (11%) (Fig. 8b) was the most prevalent, being completely absent in the east zone, which was overall featured by a scarce presence of the Proteobacteria (1%) (Fig. 8). A reasonable explanation for such finding might be due to the emphasized oligotrophy of the west area with respect to the east one, thus allowing Gammaproteobacteria to survive exploiting ions present in the rock likely for chemolithotrophic energy production (Schabereiter-Gurtner et al. 2002). Moreover, bacterial members belonging to the Pseudomonadaceae family are peculiarly proficient in forming biofilm on a vast array of surfaces (Harrison et al. 2004), therefore gaining resistance traits to diverse stressors, as those that might derive by the presence of iron oxides,

carbonates, and silicates. For instance, *Pseudomonas aeruginosa* has been described as capable of colonizing different types of silicates growing as a biofilm on mineral surfaces (Aouad et al. 2008), concomitantly stimulating iron release, and overcoming iron deficiency by producing iron scavenging molecules known as siderophores (Hersman et al. 2011). Besides, *Pseudomonas* strains have been described for their ability to precipitate calcite through biomineralization processes mediated by extracellular urease activities (Abdel-Aleem et al. 2019).

Considerations and conclusions

This work is an example of multidisciplinary investigation applied to ancient paintings sited in a humid and marine environment. The paintings of the Santa Margherita's cave in Castellammare del Golfo (Trapani, Italy) have been investigated to evaluate the main causes involved in their degradation and to individuate some specific actions to plan their restoration. The environmental monitoring assured that the conditions of temperature and humidity are quite stable during the year.

First of all, despite the long time after the paintings were done, the remains of mortars and pigments demonstrate that the execution technique and materials had good quality. Under the point of view of their conservation, the paintings are in an advanced state of deterioration, especially those in the east wall, and the painting is a complex scenario for its preservation due to the environment of the site.

The paintings were realized at secco by using poor earth pigments and egg yolk as binder, considerably degraded, on a preparation layer of mortar and the stone support made of dolomite.

The microstructure of the mortar samples indicates similarities of raw materials and production of the east and west 1 paintings; in addition it evidences a secondary production of the west 2 painting with a coarser manufacture even if more recent.

The presence of a high content of chlorine revealed a greater exposure of east wall to the sea aerosol, which caused a greater degree of damage degradation of the painting of the east wall.

Due to the high level of damage of the paintings, they require stabilization, firstly, by procedures of consolidation of both plaster and pictorial film and, secondly, by repairing the rims of the mortars in all the areas exposed. The presence of gypsum requires peculiar approaches of conservation for instance by using specific gels for the surface cleaning (Grassi et al. 2007; Carretti et al. 2007; García-Vera et al. 2020; Salvadori et al. 2003) or consolidant approaches such as the Ferroni-Dini or of the barium method (Matteini 2008; Slížková et al. 2015) or the more recent use of nanolime (Rodrigues et al. 2018.) It is worth to underline that before the restoration process a deepen study about the sulfates distribution on the whole painting layers needs to be performed.

The study of the microbiome of the east and west walls of Santa Margherita's cave demonstrated common microbial members, mainly belonging to the Bacillaceae and Planococcaceae families, likely due to their ability of colonizing environments rich of minerals, such as carbonates and silicates (Laiz et al. 2000; Randazzo et al. 2015). In addition, microbiome analysis evidenced differences among the two walls, with east wall carrying a higher abundance of Bacteroidota, probably linked with fecal animal contamination due to the close proximity of this wall to the uncontrolled entrance of the cave; contrarily, west wall contained more Proteobacteria, reasonably due to their capability of adaptation to more oligotrophic environments.

All these biotic aspects highlight microorganisms as prone and efficient in colonizing harsh and extreme environments as that represented by the case study here reported; however, considering the biochemical repertoire that bacteria can elicit in response to diverse external stresses, whether microbes can act as deteriogen or biocontrol agents is yet to be defined. Indeed, if DNA sequencing-based technology represents a powerful tool to unveil the identity of uncultivable microbes, further research is needed to deeply understand how physical–chemical and biological aspects of cave environment interplay with each other. In this regard, electron microscopy techniques and the identification of microorganisms through cultivable dependent methods could shed light on possible interactions occurring between microbiota and the stone material, as well as microbial penetration phenomena that can cause physical damage of the rock material under study (Nugari et al. 2009; Caneva et al. 2015), therefore improving the development of restoration strategies for the conservation of such a complex environmental niche.

The immediate intervention could be a physical barrier, like a gate to put at the entrance of the cave. This could avoid the problem of the presence of insects, birds, or bats.

However, the growth of bacteria could be solved, at least for few years, by using controlled release systems (Dresler et al. 2017) which inhibit the bacterial growth. In a previous paper some samples collected at the Santa Margherita cave have been treated and the efficacy of treatment was demonstrated for one year (Presentato et al. 2020a, 2020b).

At the end of the conservation work, a thin layer of protective could be applied as sacrificial layers in order to improve the hydro-repellency of the surface (Caponetti et al. 2021; Renda et al. 2020).

Supplementary Information The online version contains supplementary material available at https://doi.org/10.1007/s11356-021-17211-0.

Acknowledgements We would like to express our gratitude to Soprintendenza di Trapani for allowing us to investigate and collect samples from the paintings at Santa Margherita Cave and to thank Ignazio Sottile (BC Sicilia) for his fruitful cooperation.

The authors would like to express our gratitude to Comune di Catellammare del Golfo for the interest to the research. EC, GC, and FA thank Mr I. Sottile for useful discussions and guide us to reach the site. Thanks are due to Prof. G. Traina of the Academy of Art of Palermo for his precious suggestions about the methodology to use for the restoration of the paintings.

Eugenio Caponetti wants to dedicate this paper to the memory of prof. Sebastiano Tusa, who had inspired this work during a discussion about the conservation of paintings in Sicily caves.

Author contribution FA, EC, and MLS: Conceptualization and methodology. JC and FA: XRD, XRF, and FT-IR investigations. PdS: petrographic analysis. RA, AP and LV: biological test, bioinformatic analysis and data analysis. AS: NMR data analysis. FA, EC, MS, RA, and AP: writing–review and editing. All authors contributed to the article and approved the submitted version.

Funding A.P. and F.A thank MIUR for the Project PON Ricerca e Innovazione 2014–2020 – Avviso DD 407/2018 "AIM Attrazione e Mobilità Internazionale" (AIM1808223). This work is part of the project "Development and Application of Innovative Materials and processes for the diagnosis and restoration of Cultural Heritage—DELIAS"—PON03PE 00214 2 (Programma Operativo Nazionale Ricerca e Competitività2007–2013).

Data availability The datasets used or analyzed during the current study are available from the corresponding author on reasonable request.

Declarations

Ethics approval Not applicable. This manuscript does not involve researching about humans or animals.

Consent to participate All of the authors consented to participate in the drafting of this manuscript.

Consent to publish All of the authors consented to publish this manuscript.

Competing interests The authors declare that they have no competing interests.

References

Abdel-Aleem H, Dishisha T, Saafan A et al (2019) Biocementation of soil by calcite/aragonite precipitation using Pseudomonas azotoformans and Citrobacterfreundii derived enzymeshttps://doi.org/10.1039/C9RA02247C

Achal V, Mukherjee A, Reddy M (2011) Effect of calcifying bacteria on permeation properties of concrete structures. J Ind Microbiol Biot 38:1229–1234. https://doi.org/10.1007/s10295-010-0901-8

Albertano P (1993) Epilithic algal communities in hypogean environments. G Bot Ital 127(3):386–438

Alonso L, Pommier T, Kaufmann B et al (2019) Anthropization level of Lascaux Cave microbiome shown by regional-scale comparisons of pristine and anthropized caves. Mol Ecol 28(14):3383–3394. https://doi.org/10.1111/mec.15144

Anne S, Rozenbaum O, Andreazza P, Rouet J (2010) Evidence of a bacterial carbonate coating on plaster samples subjected to the calcite bioconcept biomineralization technique. Constr Build Mater 24:1036–1042. https://doi.org/10.1016/j.conbuildmat.2009.11.014

Aouad G, Crovisier JL, Damidot D et al (2008) Interactions between municipal solid waste incinerator bottom ash and bacteria (Pseudomonas aeruginosa). Sci Total Environ 393:385–393

Armetta F, Nardo VM, Trusso S et al (2021) The silver collection of San Gennaro treasure (Neaples): a multivariate statistic approach applied to X-ray fluorescence data. Spectrochim Acta Part B Atomic Spectroscopy 180:106171

Aubert M, Setiawan P, Oktaviana AA, Brumm A et al (2018) V Palaeolithic cave art in Borneo. Nature 564:254–257

Belfiore CM, Barca D, Bonazza A et al (2013) Application of spectrometric analysis to the identification of pollution sources causing cultural heritage damage. Environ Sci Pollut Res 20:8848–8859. https://doi.org/10.1007/s11356-013-1810-y

Callahan BJ, McMurdie PJ, Rosen MJ et al (2016) DADA2: high-resolution sample inference from Illumina amplicon data. Nat Methods 13:581–583. https://doi.org/10.1038/nmeth.3869

Caneva G, Tescari M, Bartoli F, Nugari MP, Pietrini AM, Salvadori O (2017) Ecological Mapping for the Preventive Conservation of Prehistoric Mural Paintings in Rock Habitats: the Site of Filiano (Basilicata, Italy). Conserv Sci Cult Herit 15(2):53–59. https://doi.org/10.6092/issn.1973-9494/7118

Caneva G, Tescari M, Bartoli F, Nugari MP, Pietrini AM, Salvadori O (2015). Ecological Mapping for the Preventive Conservation of Prehistoric Mural Paintings in Rock Habitats: the Site of Filiano (Basilicata, Italy). Conservation Science in Cultural Heritage 15(2):53–59. https://doi.org/10.6092/issn.1973-9494/7118

Caneva G, Bartoli F, Fontani M, Mazzeschi D, Visca P (2019) Changes in biodeterioration patterns of mural paintings: multi-temporal mapping for a preventive conservation strategy in the Crypt of the Original Sin (Matera, Italy). J Cult Herit 40:59–68

Caponetti E, Armetta F, Ciaramitaro V et al (2021) Effectiveness of some protective and self-cleaning treatment: a challenge for the conservation of the Temple G in Selinunte. Prog Surf Coat 151:106020

Carretti E, Giorgi R, Berti D, Baglioni P (2007) Oil-in-water nanocontainers as low environmental impact cleaning tools for works of art: Two case studies. Langmuir 23(11):6396–6403

Charola AE (2000) Salt in the deterioration of porous materials. J Am Inst Conserv 39:327–343

Chen Q, Liu Z, Peng Q et al. (2010) Diversity of halophilic and halotolerant bacteria isolated from non-saline soil collected from Xiaoxi National Natural Reserve, Hunan Province. 50(11):1452-9

Comite V, Álvarez de Buergo M, Barca D et al (2017) Damage monitoring on carbonate stones: field exposure tests contributing to pollution impact evaluation in two Italian sites. Constr Build Mater 152:907–922. https://doi.org/10.1016/j.conbuildmat.2017.07.048

Corral P, Amoozegar MA, Ventosa A (2020) Halophiles and their biomolecules: recent advances and future applications in biomedicine. Mar Drugs 18:33. https://doi.org/10.3390/md18010033

Corvo F, Reyes J, Valdes C et al (2010) Influence of air pollution and humidity on limestone materials degradation in historical buildings located in cities under tropical coastal climates. Water Air Soil Pollut 205:359. https://doi.org/10.1007/s11270-009-0081-1

Costa EAL, Campos VP, da Silva Filho LCP, Greven HA (2009) Evaluation of the aggressive potential of marine chloride and sulfate salts on mortars applied as renders in the Metropolitan Region of Salvador – Bahia. Brazil J Environ Manage 90:1060–1068

Coy MR, Hoffmann M, Kingdom Gibbard HN et al (2014) Nested-quantitative PCR approach with improved sensitivity for the detection of low titer levels of Candidatus Liberibacter asiaticus in

the Asian citrus psyllid Diaphorina Citri Kuwayama. J Microbiol Methods 102:15–22. https://doi.org/10.1016/j.mimet.2014.04.007
Creer KM, Kopper JS (1974) Paleomagnetic dating of cave paintings in Tito Bustillo Cave, Asturias, Spain. Science 186:348–350
De Muynck W, Verbeken K, De Belie N, Verstraete W (2013) Influence of Temperature on the Effectiveness of a Biogenic Carbonate Surface Treatment for Limestone Conservation. Appl Microbiol Biot 97:1335–1347. https://doi.org/10.1007/s00253-012-3997-0
Dhami NK, Reddy MS, Mukherjee A (2014) Application of calcifying bacteria for remediation of stones and cultural heritages. Front Microbiol 5:304. https://doi.org/10.3389/fmicb.2014.00304 4071612
Dick J, De Windt W, De Graef B, Saveyn H, Van DM, De Belie N, Verstraete W (2006) Bio-deposition of a calcium carbonate layer on degraded limestone by Bacillus species. Biodegradation 17:357–367. https://doi.org/10.1007/s10532-005-9006-x
Dresler C, Saladino ML, Demirbag C et al (2017) Development of controlled release systems of biocides for the conservation of cultural heritage. Int Biodeterior Biodegradation 125:150–156
Fairbridge R (1957) The dolomite question Regional Aspects of Carbonate Deposition Edited by Rufus. J Le Blanc and Julia g Breeding 5:125–178
Galante M (2011) La grotta Santa Margherita Ministero dell'Istruzione, dell'Università e della Ricerca Accademia di Belle Arti di Palermo.
Gaona O, Cerqueda-Garcı´a D, Falco´n LI et al (2019) Microbiota composition of the dorsal patch of reproductive male Leptonycteris yerbabuenae. PLoS One 14(12):0226239. https://doi.org/10.1371/journal.pone.0226239
García-Vera VE, Tenza-Abril AJ, Solak AM, Lanzón M (2020) Calcium hydroxide nanoparticles coatings applied on cultural heritage materials: their influence on physical characteristics of earthen plasters. Appl Surf Sci 504:144195
Grassi S, Carretti E, Pecorelli P et al (2007) The conservation of the Vecchietta's wall paintings in the Old Sacristy of Santa Maria della Scala in Siena: the use of nanotechnological cleaning agents. J Cult Herit 8(2):119–125
Hammer Ø, Harper DAT, Ryan PD (2001) PAST: Paleontological statistics software package for education and data analysis. Palaeontol Electron 4(1):9
Harrison JJ, Ceri H, Stremick C, Turner RJ (2004) Biofilm susceptibility to metal toxicity. Environ Microbiol 6:1220–1227
Helen H (2003) Pigments of English medieval wall painting archetype publications. London
Hersman LE, Huang A, Maurice PA, Jennifer H (2011) Forsythe siderophore production and iron reduction by Pseudomonas mendocina in response to iron deprivation. Geomicrobiol J 4:261–273. https://doi.org/10.1080/01490450050192965
Kim HK, Park SJ, Han JI, Lee HK (2013) Microbially mediated calcium carbonate precipitation on normal and lightweight concrete. Constr Build Mater 38:1073–1082. https://doi.org/10.1016/j.conbuildmat.2012.07.040
La Russa MF, Rovella N, Pelosi C et al (2016) A multi-analytical approach applied to the archaeometric study of mortars from the Forty Martyrs rupestrian complex in Cappadocia (Turkey). Microchem J 125:34–42
Laiz L, Recio D, Hermosin Saiz-Jimenez BC (2000) Microbial communities in salt efflorescences. In Of Microbes and Art, the Role of Microbial Communities in the Degradation and Protection of Cultural Heritage. Kluwer Academic/Plenum Publishers, New York.
Lee HS, Kim SH, Han KS (2019) Diagnosis and Evaluation of Conservation State of Mural Paintings in Payathonzu Temple on Bagan Heritage Site in Myanmar. J Conserv Sci The Korean Society of Conservation Science for Cultural Heritage 35(5):494–507. https://doi.org/10.12654/jcs.2019.35.5.10
Lu S et al (2010) Ecophysiology of Fe-cycling bacteria in acidic sediments. Appl Environ Microbiol 76:8174–8183
Ma Y, Zhang H, Du Y et al (2015) The community distribution of bacteria and fungi on ancient wall paintings of the Mogao Grottoes. Sci Rep 5:7752. https://doi.org/10.1038/srep07752
Matteini M (2008) Inorganic treatments for the consolidation and protection of stone artefacts. Conserv Sci Cult Herit 8(1):13–27. https://doi.org/10.6092/issn.1973-9494/1393
Metin S, Soslu A (2018) The Altıkapılı Cave Church at Pisidia Hüseyin. Adalya 21:311–334
Morillas H, de Mendonça F, Filho F, Derluyn H et al (2020) Decay processes in buildings close to the sea induced by marine aerosol: Salt depositions inside construction materials. Sci Total Environ 721:137687. https://doi.org/10.1016/j.scitotenv.2020.137687
Nason G, Lithgow K (1999) Environmental monitoring of the great painted staircase at Knole. The Conservator 23:57–67. https://doi.org/10.1080/01410096.1999.9995139
Nugari MP, Pietrini AM, Caneva G, Imperi F, Visca P (2009) Biodeterioration of mural paintings in a rocky habitat: The Crypt of the Original Sin (Matera, Italy). Int Biodeterior Biodegradation 63(6):705–711
Pavlik I, Gersl M, Bartos M et al (2018) Nontuberculous mycobacteria in the environment of Hranice Abyss, the world's deepest flooded cave (Hranice karst, Czech Republic). Environ Sci Pollut Res 25:23712–23724. https://doi.org/10.1007/s11356-018-2450-z
Petrushkova JP, Lyalikova NN (1986) Microbiologial degradation of lead-containing pigments in mural paintings. Stud Conserv 31:65–69
Piacenza E, Presentato A, Di Salvo F et al (2020) A combined physical–chemical and microbiological approach to unveil the fabrication, provenance, and state of conservation of the Kinkarakawa-gami art. Sci Rep 10:16072. https://doi.org/10.1038/s41598-020-73226-6
Pietrini AM, Ricci S, Nugari MP (2008) Churches and crypts. In: Caneva G, Nugari MP, Salvadori O (eds) Plant Biology for Cultural Heritage. Biodeterioration and Conservation. Getty Conservation Institute, New York, pp 179–183
Portillo MC, Gonzalez JM, Saiz-Jimenez C (2008) Metabolically active microbial communities of yellow and grey colonizations on the walls of Altamira Cave. Spain. J Appl Microbiol 104(3):681–91. https://doi.org/10.1111/j.1365-2672.2007.03594.x
Presentato A, Armetta F, Spinella A et al. (2020) Formulation of mesoporous silica nanoparticles for controlled release of antimicrobials for stone preventive conservation Frontiers in Chemistry 8:699. Manuscript ID: 555668https://doi.org/10.3389/fchem.2020.00699
Presentato A, Lampis S, Vantini A et al (2020) On the Ability of Perfluorohexane Sulfonate (PFHxS) Bioaccumulation by Two Pseudomonas sp. Strains Isolated from PFAS-Contaminated Environmental Matrices. Microorganisms 8:92
Pruesse E, Peplies J, Glockner FO (2012) SINA: Accurate high-throughput multiple sequence alignment of ribosomal RNA genes. Bioinformatics 28(14):1823–1829. https://doi.org/10.1093/bioinformatics/bts252
Purpura G (1999) Le pitture della grotta di Santa Margherita, Kalos – L'arte in Sicilia. Kalos 6:30
Randazzo L et al (2015) Flos Tectorii degradation of mortars: An example of synergistic action between soluble salts and biodeteriogens. J Cult Herit 16:838–847
Meilunas RJ, Bentsen JG, Steinberg A (1993) Analysis of Aged Paint Binders by FTIR Spectroscopy. Stud Conserv 35:33–51
Remmas N, Melidis P, Voltsi C, Athanasiou D, Ntougias S (2017) Novel hydrolytic extremely halotolerant alkaliphiles from mature landfill leachate with key involvement in maturation process. J Environ Sci Health A Tox Hazard Subst Environ Eng 52(1):64–73. https://doi.org/10.1080/10934529.2016.1229931

Renda V, Alvarez de Buergo M, Saladino ML, Caponetti E (2020) Assessment of protection treatments for carbonatic stone using nanocomposite coatings". Prog Org Coat 141:105515

Renda V, Mollica Nardo V, Anastasio G, Caponetti E, Vasi CS, Saladino ML, Armetta F, Trusso S, Ponterio RC (2019) A multivariate statistical approach of X-ray fluorescence characterization of a large collection of reverse glass paintings Spectrochimica Acta - Part B Atomic SpectroscopyVolume 159:105655

Rizzo G, Ercoli L, Parlapiano M (2008) Characterization of mortars from ancient and traditional, water supply systems in Sicily. J Therm Anal Calorim 92(1):323–330

Roccardi A, Ricci S, Pietrini AM (2008) Semienclosed environments. In: Caneva G, Nugari MP, Salvadori O (eds) Plant Biology for Cultural Heritage Biodeterioration and Conservation. Getty Conservation Institute, New York, pp 206–210

Rodrigues JD, Ferreira Pinto AP, Nogueira R, Gomes A (2018) Consolidation of lime mortars with ethyl silicate, nanolime and barium hydroxide Effectiveness Assessment with Microdrilling data. J Cult Herit 29:43–53

Rossi M, Galizzi A, Mastromei G, et al (2006) Bacillus subtilis gene cluster involved in calcium carbonate biomineralization Chiara Barabesi. J Bacteriol 189(1):228–235. https://doi.org/10.1128/JB.01450-06

Russ J, Pohl D, M, L von Nagy C, et al (2017) Strategies for 14C Dating the Oxtotitlán Cave Paintings, Guerrero, Mexico. Adv Archaeol Pract 5:170–183

Salvadori B, Errico V, Mauro M, Melnik E, Dei L (2003) Evaluation of Gypsum and Calcium Oxalates in Deteriorated Mural Paintings by Quantitative FTIR Spectroscopy. Spectrosc Lett 36(5–6):501–513

Saunders D, Kirby J (2004) The Effect of Relative Humidity on Artists' Pigments. National Gallery Technical Bulletin 25:62–72

Scatigno C, Gaudenzi S, Sammartino MP, Visco G (2016) A microclimate study on hypogea environments of ancient roman building. Sci Total Environ 566–567:298–305

Schabereiter-Gurtner C, Piñar G, Vybiral D, Lubitz W, Ro¨lleke S (2001) *Rubrobacter*-related bacteria associ- ated with rosy discolouration of masonry and lime wall paintings. Arch Microbiol 176(5):347–354. https://doi.org/10.1007/s002030100333

Schabereiter-Gurtner C, Saiz-Jimenez C, Pinar G et al (2002) Phylogenetic 16S rRNA analysis reveals the presence of complex, partly unknown bacterial communitiesin Ttito bustillo cave, Spain, on its palaeolithic paintings. Environ Microbiol 4:392–400

Slížková Z, Drdácký M, Viani A (2015) Consolidation of weak lime mortars by means of saturated solution of calcium hydroxide or barium hydroxide. J Cult Herit 16(4):452–460

Sofia S, Elini K, Anglos D, Spyros A (2014) Egg yolk identification and aging in mixed paint binding media by NMR spectroscopy. John Wiley & Sons, Ltd

Spyros A, Anglos D (2006) Studies of organic paint binders by NMR spectroscopy. Applied Physics A. Materials Science & Processing A 83:705–508

Stefanis NA, Theoulakis P, Pilinis C (2009) Dry deposition effect of marine aerosol to the building stone of the medieval city of Rhodes, Greece. Build Environ 44(2):260–270

Sun DL, Gao YZ, Ge XY, Shi ZL, Zhou NY (2020) Special Features of Bat Microbiota Differ From Those of Terrestrial Mammals. Front Microbiol 11:1040. https://doi.org/10.3389/fmicb.2020.01040

Takahashi S, Tomita J, Nishioka K, Hisada T, Nishijima M (2014) Development of a prokaryotic universal primer for simultaneous analysis of Bacteria and Archaea using next-generation sequencing. PLoS One 9(8):105592. https://doi.org/10.1371/journal.pone.0105592

Tascon M, Mastrangelo N, Gallegos D, Marte F (2017) Determination of materials and techniques involved in the mural paintings of San Miguel Church, Argentina. J Raman Spectrosc 48:1356–1364

Tomaselli L, Lamenti G, Bosco M, Tiano P (2000) Biodiversity of photosynthetic micro-organisms dwelling on stone monuments. Int Biodeterior Biodegradation 46:251–258

Tortora M, Sfarra S, Chiarini M et al (2016) Non-destructive and micro-invasive testing techniques for characterizing materials, structures and restoration problems in mural paintings. Appl Surf Sci 387:971–985

Vahur S, Teearu A, Peets P, Joosu L, Leito I (2016) ATR-FT-IR spectral collection of conservation materials in the extended region of 4000–80 cm^{-1}. Anal Bioanal Chem 408:3373–3379

Vettori S, Bracci S, Cantisani E et al (2016) A multi-analytical approach to investigate the state of conservation of the wall paintings of Insula 104 in Hierapolis (Turkey). Microchem J 128:279–287

Walujkar SA et al (2019) Utilizing the iron tolerance potential of Bacillus species for biogenic synthesis of magnetite with visible light active catalytic activity. Colloid Surf B 177:470–478

Yasir M (2018) Analysis of bacterial communities and characterization of antimicrobial strains from cave microbiota. Braz J Microbiol 49(2):248–257. https://doi.org/10.1016/j.bjm.2017.08.005

Zhang G, Gong C, Gu J, Katayama Y, Someya T, Gu JD (2019) Biochemical reactions and mechanisms involved in the biodeterioration of stone world cultural heritage under the tropical climate conditions International. Biodeterior Biodegradation 143:10472